Michael Langenmaier and Caroline Röhr*

The new sodium tellurido manganates(II) $Na_2Mn_2Te_3$, $Na_2Mn_3Te_4$, Na_2AMnTe_3 (A = K, Rb), and $NaCsMnTe_2$

https://doi.org/10.1515/znb-2019-0104
Received July 1, 2019; accepted August 4, 2019

Abstract: A series of new sodium and mixed Na/A (A = K, Rb, Cs) tellurido manganates have been synthesized from melts of the pure elements (or MnTe) at maximum temperatures of 600–1000°C. The monoclinic crystal structures of the two pure sodium salts $Na_2Mn_2Te_3$ (space group $C2/c$, a = 1653.68(2), b = 1482.57(2), c = 773.620(10) pm, β = 117.52°, Z = 8, $R1$ = 0.0225) and $Na_2Mn_3Te_4$ (space group $C2/m$, a = 1701.99(3), b = 438.741(8), c = 691.226(12) pm, β = 90.3171(8)°, Z = 2, $R1$ = 0.0270) are both based on a hexagonal close packed Te^{2-} arrangement. $Na_2Mn_2Te_3$ is isotypic with $Na_2Mn_2S_3$ and $Na_2Mn_2Se_3$ and contains layers of $[MnTe_4]$ tetrahedra, which are connected *via* common edges to form tetramers $[Mn_4Te_6]$. These tetramers are further connected *via* μ_3-Te atoms. $Na_2Mn_3Te_4$ crystallizes in a new structure type, recently also reported for the selenido salt $Na_2Mn_3Se_4$. Mn(2) forms ribbons of vertex-sharing dinuclear units $^1_\infty[Te_{2/2}MnTe_2MnTe_{2/2}]$ running along the short b axis of the monoclinic cell. The Te atoms of these ribbons are also the ligands of edge-sharing $[Mn(1)Te_6]$ chains of octahedra. Similar to $Na_2Mn_2Te_3$, the Na^+ cations are octahedrally coordinated and the cations occupy tetrahedral (Mn^{2+}) and octahedral (Na^+, Mn^{2+}) voids in the close Te^{2-} packing. The isotypic K/Rb salts Na_2AMnTe_3 crystallize in a new structure type (orthorhombic, space group $Pmc2_1$, a = 1069.70(4)/1064.34(2), b = 1350.24(5)/1350.47(3), c = 1238.82(4)/1236.94(3) pm, Z = 4, $R1$ = 0.0445/0.0210). In contrast to the simple formula indicating a Mn(III) compound, the complex structure contains one layer consisting of undulated chains of edge-sharing tetrahedra $^1_\infty[Mn^{II}Te_{4/2}]$ separated by free ditelluride dumbbells $[Te_2]^{2-}$ and a second layer containing a complex chain of edge- and vertex-sharing $[Mn^{II}Te_4]$ tetrahedra, in which Mn(II) is coordinated to μ_1- and μ_2-Te^{2-} ligands and an η^1-ditellurido ligand. The cesium salt $NaCsMnTe_2$ (orthorhombic, space group $Cccm$, a = 694.21(2), b = 1536.57(4), c = 664.47(2) pm, Z = 4, $R1$ = 0.0131) likewise forms a new structure type, which is an ordered superstructure of $ThCr_2Si_2$. Linear chains $^1_\infty[MnTe_{4/2}]$ of edge-sharing tetrahedra are connected with similar chains $^1_\infty[NaTe_{4/2}]$ to form $[NaMnTe_2]$ layers. The larger alkali cations Cs^+ between the layers exhibit a cubic (CN = 8) coordination.

Keywords: manganese; sodium; tellurido manganates; tellurium.

1 Introduction

Mixed-valent alkali sulfido/selenido/tellurido ferrates(II/III) $A_{1-2}FeQ_2$ are a multifaceted long-known [1–3], but still growing [4–7] compound class, which exhibits a diverse crystal chemistry and therewith several interesting physical, in particular magnetic, properties. Depending on the ratio Fe^{II}:Fe^{III} and the size of the counter cations, their structures either contain (differently undulated) chains $^1_\infty[FeQ_{4/2}]$ of edge-sharing tetrahedra (cf. e.g. [3, 4, 8–10]) or the prominent cubane-type clusters $[Fe_4Q_8]$ [5, 6, 11]. In contrast, most of the analogous cobaltates ([12] and references therein) and manganates (see below) comprise divalent metal ions only. Attempts to oxidize these metal cations e.g. with an excess of sulfur, yielded complex phases like e.g. Na_3CoS_3 [12], which is not a cobaltate(III) but contains di-sulfido ligands coordinated to Co(II).

Similar to the ferrates(II/III), the structural chemistry of the manganates(II/III) is characterized by $[MnQ_4]$ tetrahedra connected predominately *via* common edges. The connectivity of these polyhedra reaches from isolated $[MnQ_4]$ tetrahedra to chains $^1_\infty[MnQ_{4/2}]$ and finally different types of 'defect' layers. In this latter case, the basic layer type differs for the smaller Li^+ and Na^+ compared to the larger K^+, Rb^+ and Cs^+ cations. $[MnQ_6]$ octahedra are very rare among the S/Se/Te manganates, but occur in the binary border phases MnQ (NaCl and/or NiAs type).

The compositions of known chalcogenido manganates(II) are restricted mainly to the four compositions (for A:Mn:Q) 6:1:4 (A = Na–Cs), 2:1:2 (K–Cs only), 2:2:3

***Corresponding author: Caroline Röhr,** Institut für Anorganische und Analytische Chemie, Universität Freiburg, Albertstrasse 21, D-79104 Freiburg, Germany, e-mail: caroline@ruby.chemie.uni-freiburg.de
Michael Langenmaier: Institut für Anorganische und Analytische Chemie, Universität Freiburg, Albertstrasse 21, D-79104 Freiburg, Germany

(Na^+ only) and 2:3:4. For the lighter alkali elements sodium and potassium, all ortho manganates A_6MnQ_4 have long been known [13, 14]. Only recently, the structural chemistry was extended by the successful preparation and characterization of the whole series of the respective rubidium and cesium salts, which are isotypic to the Na/K compounds (Na_6ZnO_4-type, [15]). The heavier alkali cations K, Rb and Cs form the whole series of sulfido, selenido and tellurido manganates(II) A_2MnQ_2 [8], which crystallize without exception in the orthorhombic K_2ZnO_2-type structure containing linear chains of tetrahedra [$MnQ_{4/2}$]. The layered manganates(II) with the smaller Li and Na counter cations can be derived from the layers of tetrahedra of the $CaAl_2Si_2$-type structure, where tetrahedral voids between every second hexagonal close packed layers of anions are occupied by Mn. $Na_2Mn_2S_3$ [16] and $Na_2Mn_2Se_3$ [17] are isotypic and crystallize in a singular monoclinic structure, in which Mn^{2+} cations occupy ⅔ of the tetrahedral voids between two close packed sulfide/selenide layers. The yet missing isotypic tellurido manganate $Na_2Mn_2Te_3$ is added herewith. $Na_2Mn_3Se_4$ [18] and the tellurium analog $Na_2Mn_3Te_4$, which is also presented in this work, differ in containing also [MnQ_6] octahedra as building blocks. The only potassium salt with this composition is the sulfido salt $K_2Mn_3S_4$. It forms a singular monoclinic structure [19, 20], which is certainly related to the common $Cs_2Mn_3S_4$-type structure of the Rb and Cs compounds $A_2M_3Q_4$ (Q = S, Se, Te; [21]). The named manganates(II) contain Mn^{II} ions in a HS-d^5 configuration. Their magnetic structures, if known, are dominated by an anti-ferromagnetic (AFM) ordering, with magnetic moments close to the spin-only value [13–15, 18, 22].

The layered structures of the Li and Na compounds offer the opportunity for electrochemical modifications: for example, mixed alkali compounds were obtained by an oxidative deintercalation (i.e. partial oxidation of Mn^{II}) followed by a reductive intercalation [23].

Compounds containing manganese(III) are comparatively rare and are obtained for Se and Te only. The structure of the mixed-valent tellurido phase $NaMn_{1.56}Te_2$ exhibits a statistic occupation of the tetrahedral voids in an h.c.p. arrangement of tellurium ions [24]. The pure Li and Na manganates(III) AMnSe$_2$ [17] and AMnTe$_2$ [25] as well as the mixed-valent phase $Na_3Mn_4Te_6$ (25% Mn^{III}, [24]) likewise contain h.c.p. chalcogen arrangements with layer-wise Mn-filled tetrahedral voids. Whereas these Li/Na compounds were directly obtained from melts of the elements, the synthesis of the K, Rb and Cs salts AMn(Se/Te)$_2$ (TlAgTe$_2$-type [17, 24]) requires starting from pre-synthesized LiMnQ_2 and the respective alkali chloride [17]. Their likewise layered chalcogenido metallate anions resemble the HgI_2-type structure and thus contain – in contrast to the others – vertex-sharing tetrahedra. For the named tellurido phases, the oxidation state of manganese has been proven by magnetic measurements [24]. More recently, these chalcogenido salts containing d^4-Mn^{III} gained some attraction due to their half-metallic ferromagnetic properties, which are potentially applicable for spintronic devices [26, 27].

In the course of our systematic studies on the crystal chemistry of mixed-valent chalcogenido metallates(II/III) of iron, cobalt and manganese, the new sodium tellurido manganates(II) $Na_2Mn_2Te_3$ and $Na_2Mn_3Te_4$ (cf. also [28]) as well as the mixed Na–A (A = K, Rb) salts Na_2AMnTe$_3$ and NaCsMnTe$_2$ were obtained from melts of the elements with Mn or MnTe as manganese source. Whereas the two pure sodium manganates are built up of close packed layers of chalcogenide ions Q^{2-} and NaCsMnTe$_2$ is also structurally related to the already known compounds, the mixed A_3MnTe$_3$-type phases with Na/K and Na/Rb exhibit very complex new structures with motifs resembling those of the cobaltate(II) Na_3CoS_3 [12].

2 Experimental

2.1 Preparation and phase analysis

The new sodium tellurido manganates(II) were synthesized in corundum crucibles sealed in steel autoclaves under an argon atmosphere. Starting materials were the pure alkali metals (Na, K: Merck, >99%; Rb, Cs: 99.99%) MnTe (powder, ABCR GmbH, Karlsruhe, 99.9%) or elemental Mn as source of manganese and a corresponding amount of the elemental tellurium (shots, ABCR GmbH, Karlsruhe). Due to the violent reactions, cautious heating rates $\dot{T}^{\uparrow}$ like e.g. 5 K h^{-1} (between 80 and 110°C) were applied. Subsequently after reaching the maximum temperatures (T_{max}) of 600–1000°C, the samples were slowly cooled down to r.t. After the preparations, representative parts of the reguli were ground and sealed in capillaries with a diameter of 0.3 mm. X-ray powder diagrams were collected on transmission powder diffractometer systems (Stoe STADI-P with linear PSD or Dectris Mythen 1K strip detector, MoK_α radiation, graphite monochromator). For the phase analysis, the measured powder diagrams were compared to the calculated (program Lazy-Pulverix [29]) reflections of the target compounds and other known phases in the respective systems Na–(K/Rb/Cs)–Mn–Te.

In the ternary system Na–Mn–Te several samples were prepared primarily with the focus to obtain new

mixed-valent Mn(II/III) compounds. Several samples of the overall composition $Na_3Mn_4Te_6$, which is one of the very rare mixed-valent tellurido manganates reported in the literature [24], were heated to different maximum temperatures. In a first attempt to reproduce this compound directly starting from the pure elements [46.3 mg (2.01 mmol) Na, 145.3 mg (2.645 mmol) Mn and 510.6 (4.002) Te] a maximum temperature of 900°C has been applied, which was reached after several heating steps [$\xrightarrow{20}90\xrightarrow{4}110\xrightarrow{100}420\xrightarrow{20}480\xrightarrow{250}900$ ($\dot{T}^{\uparrow}$ in K h^{-1} and T in °C)]. Subsequent cooling with rates of 250 (down to 700°C) and 20 K h^{-1} down to r.t. yielded the new compound $Na_2Mn_3Te_4$ instead of $Na_3Mn_4Te_6$, together with small amounts of $MnTe_2$. Whereas an analogous sample with a maximum temperature of 700°C also gave this new phase, a further reduced T_{max} of 600°C led to the formation of the known mixed-valent compound $Na_3Mn_4Te_6$ (according to the phase analysis by powder X-ray diffraction together with $NaTe_3$, MnTe and $MnTe_2$). This critical maximum temperature agrees with the synthesis of $Na_3Mn_4Te_6$ as reported by Kim et al. [24], who obtained this phase keeping stoichiometric amounts of the elements in niobium ampules at 600°C for 1 week. The second pure sodium tellurido manganate, $Na_2Mn_2Te_3$, was obtained from a Te-rich sample of the composition Na_3MnTe_6, for which 38.1 mg (1.66 mmol) sodium, 104.5 mg (0.573 mmol) MnTe and 361.2 mg (2.831 mmol) tellurium were heated up with a similar temperature program as detailed above to a maximum temperature of 1000°C. The cooling rates were 250 K h^{-1} to 800°C and finally again 20 K h^{-1} to r.t. The powder diagram of this sample shows the additional formation of $Na_3Mn_4Te_6$ and, due to the high tellurium excess not surprising, $NaTe_3$. Both new sodium compounds form dark-red platelike crystals.

In attempts to obtain new chain/cluster compounds with compositions close to A_2MnQ_2 mixtures of alkali cations A of different size were used. The respective sample $NaKMnTe_2$ consisting of 43.2 mg (1.88 mmol) Na, 73.8 mg (1.89 mmol) K, 344.9 mg (1.890 mmol) MnTe and 239.6 mg (1.878 mmol) Te, was heated with 20 K h^{-1} to 80°C and subsequently with 200 K h^{-1} to a T_{max} of 760°C. Cooling with a rate of 10 K h^{-1} to r.t. yielded the first specimen of the new compounds Na_2AMnTe_3. In accordance with the excess of potassium, the known K-rich phase K_2MnTe_2 [8] was identified as a by-product in the X-ray powder diagram of this sample. The analogous sample containing the heavier alkali element rubidium, $NaRbMnTe_2$, yielded only a mixture of already known ternary compounds (Rb_2MnTe_2 [8], Na_6MnTe_4 [13] and $RbMnTe_2$ [24]). The isotypic Rb analog $Na_2RbMnTe_2$ could finally be obtained in pure phase from a stoichiometric sample [224.9 mg (9.783 mmol) Na, 418.7 mg (4.899 mmol) Rb, 894.2 mg (4.899 mmol) MnTe and 1243.7 mg (9.747 mmol) Te] at a maximum temperature of 800°C, when applying a slow cooling rate of 5 K h^{-1} between 650 and 100°C. Attempts to synthesize the cesium derivative of this type [sample $Na_2CsMnTe_3$: 40.9 mg (1.78 mmol) Na, 120.4 mg (0.906 mmol) Cs, 167.4 mg (0.917 mmol) MnTe and 234.4 mg (1.837 mmol) Te, T_{max} = 800°C] yielded (together with Na_6MnTe_4) the new compound $NaCsMnTe_2$, which could be finally obtained in pure phase from a stoichiometric sample $NaCsMnTe_2$ [27.1 mg (1.18 mmol) Na, 151.7 mg (1.141 mmol) Cs, 208.0 mg (1.140 mmol) MnTe and 146.0 mg (1.144 mmol) Te] at the same maximum temperature (cooling rate $\dot{T}^{\downarrow} = 10\ K^{-1}$ from 650°C to r.t.). Similar to the pure sodium phases, the mixed Na-(K/Rb/Cs) tellurido manganates also form dark-red crystals, which are very sensitive against moisture.

2.2 Crystal structure determinations

For the single crystal structure analyses of the title compounds, the dark-red crystals were selected and fixed in loop sample holders (100 K measurements) or in glass capillaries (⌀ < 0.1 mm) under dried paraffin oil. Data sets were collected on a diffractometer equipped with a microsource and a CCD detector (Bruker APEX II Quazar, Mo radiation, 100 K) or on a sealed tube image plate detector system (Stoe IPDS-2, Ag radiation, r.t.).

$Na_2Mn_2Te_3$: The reflections on the diffraction images collected at 100 K could be indexed with a monoclinic *C*-centered lattice with lattice parameters resembling those of the sulfido and selenido compounds $Na_2Mn_2Q_3$. The additional reflection condition $0kl$: $k+l=2n$ is also compatible with the space group $C2/c$ of these structures. The refinement of the positional and ADP parameters of the $Na_2Mn_2S_3$ structure model [16] using the program Shelxl-2013 [30] smoothly converged to a residual value $R1$ of 0.0225. The results of this refinement are collected in the Tables 1 (first row) and 2 [35].

$Na_2Mn_3Te_4$: The lattice parameters and the general reflection conditions of the single crystal data of $Na_2Mn_3Te_4$ allowed the assignment of the possible monoclinic space groups $C2/m$, Cm and $C2$. The structure solution by Direct Methods (program Shelxs-2013 [30]) was successful in the centrosymmetric space group $C2/m$ and yielded one sodium, two Mn and two Te positions. The standardized (Structure Tidy [36]) parameters were refined as described for $Na_2Mn_2Te_3$ above and led again to a satisfactorily low $R1$ value of 0.0270. However, the refined ADP parameters of the octahedrally coordinated manganese atom Mn(1) at the origin of the unit cell describe an

Table 1: Crystallographic data and details of the data collection and structure determination for the five new tellurido manganates(II).

Compound	$Na_2Mn_2Te_3$	$Na_2Mn_3Te_4$	Na_2KMnTe_3	$Na_2RbMnTe_3$	$NaCsMnTe_2$
Structure type	$Na_2Mn_2S_3$ [16]	$Na_2Mn_3Te_4$ [28]	New	New	New
Crystal system	Monoclinic		Orthorhombic		
Space group	$C2/c$, no. 15	$C2/m$, no. 12	$Pmc2_1$, no. 26		$Cccm$, no. 66
Temperature, K	100		r.t.	100	
Lattice parameters, pm, deg					
a	1653.68(2)	1701.99(3)	1069.70(4)	1064.34(2)	694.21(2)
b	1482.57(2)	438.741(8)	1350.24(5)	1350.47(3)	1536.57(4)
c	773.620(10)	691.226(12)	1238.82(4)	1236.94(3)	664.47(2)
β	117.52	90.3171(8)			
Volume of the unit cell, 10^6 pm^3	1682.09(4)	516.15(2)	1789.29(11)	1777.93(7)	708.79(3)
Z	4	2	8	8	4
Density (X-ray), g cm^{-3}	4.25	4.64	3.88	4.25	4.37
Diffractometer	Bruker AXS Quazar		Stoe IPDS2	Bruker AXS Quazar	
Radiation	MoK_α		AgK_α	MoK_α	
Absorption coefficient μ_{Mo/AgK_α}, mm^{-1}	13.2	14.7	6.1	16.6	14.9
θ range, deg	2.0–36.6	4.8–40.9	1.5–25.6	1.5–36.5	2.7–35.3
No. of reflections collected	16 892	7495	31 227	48 797	5954
No. of independent reflections	3808	1575	7177	7975	739
R_{int}	0.0178	0.0125	0.0585	0.0246	0.0130
Corrections	Lorentz, polarisation, absorption				
	Multi-Scan [31]		Xshape [32]	Multi-Scan [31]	
Structure solution	Direct methods (Shelxs-97 [33])				
Structure refinement	Shelxl-97 [34]				
No. of free parameters	165	29	148	148	17
Goodness-of-fit on F^2	1.091	1.120	1.054	1.068	1.191
Flack x	–	–	0.01(8)	−0.001(3)	–
R values [for refl. with $I > 2\sigma(I)$]					
$R1$	0.0225	0.0270	0.0445	0.0210	0.0131
$wR2$	0.0499	0.0638	0.0795	0.0434	0.0254
R values (all data)					
$R1$	0.0250	0.0282	0.0557	0.0227	0.0135
$wR2$	0.0507	0.0644	0.0826	0.0437	0.0255
Residual elect. density, e$^-\times10^{-6}$ pm^{-3}	+3.1/ – 1.8	+2.7/ – 5.9	+1.4/ – 1.4	+3.5/ – 1.3	+1.2/ – 1.3

Table 2: Atomic coordinates and equivalent isotropic displacement parameters/pm^2 for the crystal structure of $Na_2Mn_2Te_3$.

Atoms	Wyckoff position	x	y	z	U_{eq}
Na(1)	4e	0	0.27885(11)	1/4	136(3)
Na(2)	4e	0	0.56632(11)	1/4	136(3)
Na(3)	8f	0.11176(10)	0.08308(8)	0.1565(2)	217(3)
Mn(1)	8f	0.31142(3)	0.23876(3)	0.23331(6)	91.8(7)
Mn(2)	8f	0.21214(3)	0.42020(2)	0.29194(6)	90.7(7)
Te(1)	8f	0.35221(2)	0.07610(2)	0.43314(2)	79.3(4)
Te(2)	8f	0.12821(2)	0.27893(2)	0.04236(2)	94.4(4)
Te(3)	8f	0.10690(2)	0.11465(2)	0.54977(3)	127.3(4)

ellipsoid elongated towards the Te(2) ligands [max./min. r.m.s. values: 913(15) and 127(5) pm^2]. A detailed analysis of the electron density distribution at this special position with the help of difference electron density maps calculated and visualized with the programs Jana2006 [37] and DrawXTL [38] (cf. Fig. 1a and b) indicated a small displacement of this Mn atom from its special position. Thus, equivalent alternatives for the structure refinement are (i) the application of a structure model in the acentric subgroup Cm together with a 1:1 inversion twin, (ii) the refinement of a Mn(1) split position in the centrosymmetric space group $C2/m$ or (iii) an anharmonic treatment of the Mn(1) site applying a higher ADP tensor for this atom. Due to the only small deviation of Mn(1) from the special position 2a and the only marginal improvements of the R values and residual densities in the F_o–F_c map, the final structure refinement included herein (Tables 1 and 4, [35]) is the simple harmonic anisotropic refinement in the centrosymmetric space group $C2/m$. The electron density minimum in the F_o–F_c map of −5.9 e$^-\times10^{-6}$ pm^{-3}, which lies in the direct vicinity of Mn(1), is a consequence of this choice. A similar small disorder of the octahedrally

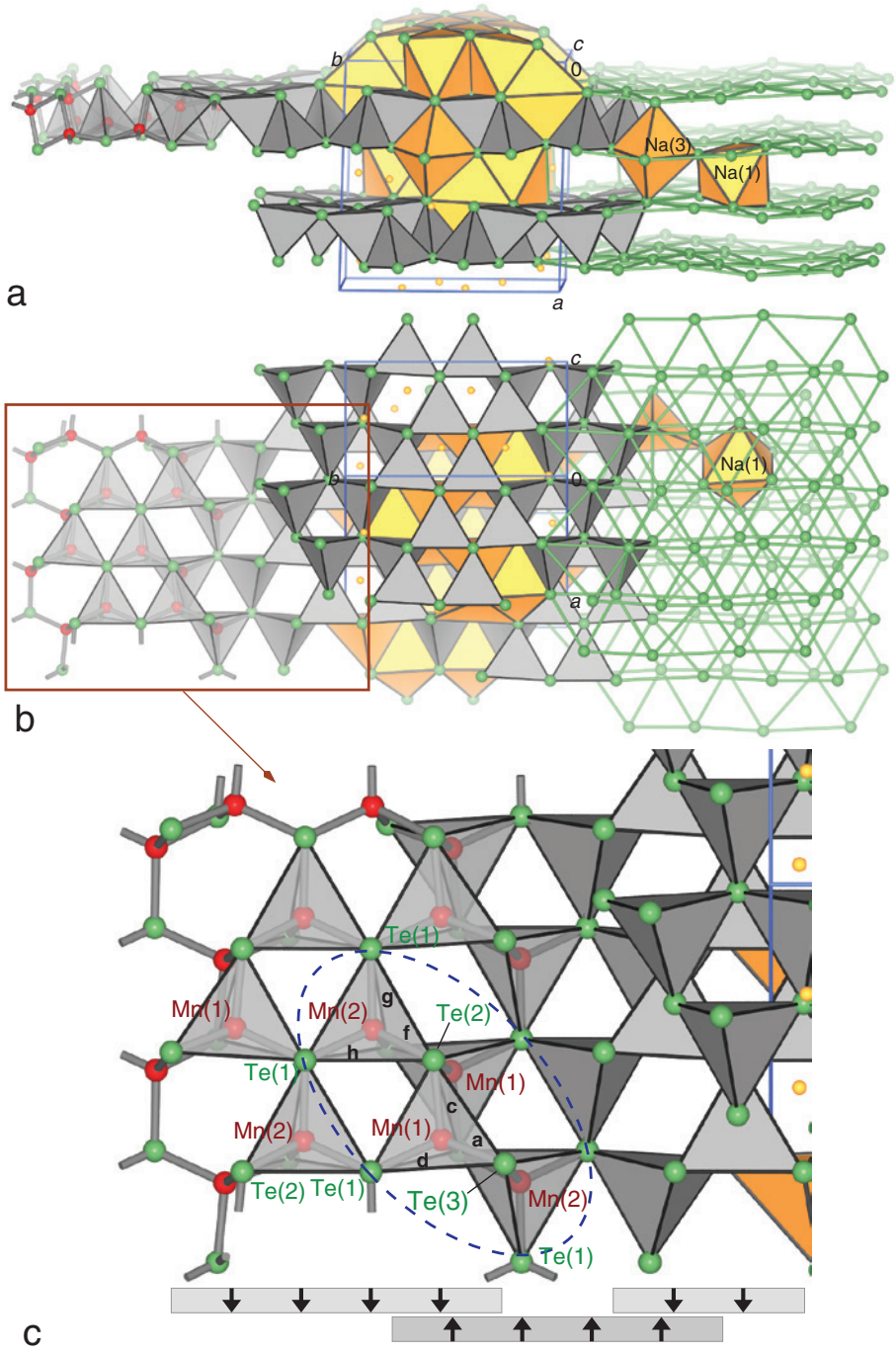

Fig. 1: Crystal structure of $Na_2Mn_2Te_3$ ($Na_2Mn_2S_3$-type). (a) Perspective view of the unit cell with a single tellurido manganate sheet extended to the left and the Te nets to the right; (b) projection of the subfigure a along (100); (c) details of the layers of [$MnTe_4$] tetrahedra (cf. Table 3 for the interatomic distances; gray polyhedra: [$MnTe_4$] tetrahedra; yellow polyhedra: [$NaTe_{5,6}$] coordination polyhedra; red/yellow/green spheres: Mn/Na/Te; program DRAWXTL [38]).

coordinated Mn(1) cations was very recently described for the isotypic selenido compound $Na_2Mn_2Se_3$ [17].

Na_2AMnTe_3: The diffraction images of crystals of the two compounds Na_2KMnTe_3 and $Na_2RbMnTe_3$ exhibit *mmm Laue* symmetry. The only additional reflection condition $h0l$: $l = 2n$ leads uniquely to the acentric space group $Pmc2_1$. The structure solution, using the methods and programs described above, yielded all 10 tellurium positions, the four manganese and the two heavier alkali sites. The positions of the overall five crystallographically different sodium cations were extracted from difference electron density maps. The conclusive *Flack*

Table 3: Selected interatomic distances (pm) and coordination numbers in the crystal structure of $Na_2Mn_2Te_3$.

Atoms		Distance	Label	Mult.	CN	Atoms		Distance	Label	Mult.	CN	Atoms		Distance	Label	CN
Na(1)	– Te(2)	319.7(1)		2×		Na(2)	– Te(2)	323.2(1)		2×		Na(3)	– Te(3)	303.7(1)		
	– Te(3)	326.2(1)		2×			– Te(1)	330.2(1)		2×			– Te(2)	308.3(1)		
	– Te(1)	332.7(1)		2×	6		– Te(1)	334.7(1)		2×	6		– Te(3)	311.5(2)		
													– Te(3)	324.2(1)		
													– Te(1)	354.1(1)		5
Mn(1)	– Te(3)	269.6(1)	**a**			Mn(2)	– Te(3)	270.8(1)	**e**							
	– Te(2)	275.3(1)	**b**				– Te(2)	275.0(1)	**f**							
	– Te(2)	275.3(1)	**c**				– Te(1)	278.4(1)	**g**							
	– Te(1)	277.4(1)	**d**		4		– Te(1)	279.2(1)	**h**	4						
	– Mn(1)	323.9(1)														
Te(1)	– Mn(1)	277.4(1)	**d**			Te(2)	– Mn(2)	275.0(1)	**f**			Te(3)	– Mn(1)	269.6(1)	**a**	
	– Mn(2)	278.4(1)	**g**				– Mn(1)	275.3(1)	**b**				– Mn(2)	270.8(1)	**e**	
	– Mn(2)	279.2(1)	**h**				– Mn(1)	275.3(1)	**c**				– Na(3)	303.7(1)		
	– Na(2)	330.2(1)					– Na(3)	308.3(1)					– Na(3)	311.5(2)		
	– Na(1)	332.7(1)					– Na(1)	319.7(1)					– Na(3)	324.2(1)		
	– Na(2)	334.7(2)					– Na(2)	323.2(1)			3 + 3		– Na(1)	326.2(1)		2 + 4
	– Na(3)	354.1(1)			3 + 4											

Table 4: Atomic coordinates and equivalent isotropic displacement parameters/pm² for the crystal structure of $Na_2Mn_3Te_4$.

Atoms	Wyckoff position	*x*	*y*	*z*	U_{eq}
Na	4*i*	0.20004(12)	0	0.2459(4)	246(5)
Mn(1)	2*a*	0	0	0	518(6)
Mn(2)	4*i*	0.41676(4)	0	0.37553(9)	115.8(10)
Te(1)	4*i*	0.56540(2)	0	0.23192(4)	118.7(6)
Te(2)	4*i*	0.16249(2)	0	0.75333(4)	128.2(6)

parameters support the non-centrosymmetric structure and the absence of twins. A noticeable Na–(K/Rb) (statistical) exchange at the overall seven cation positions is not observed. For the final refinement, the atomic coordinates were standardized and a consistent labeling of the manganese and tellurium atoms was applied (cf. Structure description). The final crystal data are collected in two intermediate columns of Table 1 and in Table 6 (see also [35]).

$NaCsMnTe_2$: The dark-red crystals of the Cs compound $NaCsMnTe_2$ also exhibit an orthorhombic, in this case small and *C*-centered, unit cell. The two further reflection conditions (0*kl*: $l = 2n$ and *h*0*l*: $l = 2n$) allowed for two different space groups, the centrosymmetric *Cccm* and the acentric *Ccc*2 group. The structure was solved and completed (Na position) as described above in the space group *Cccm*. Similar to the K and Rb compounds Na_2AMnTe_3, the distribution of the two different alkali cations is distinct, hints to a statistic distribution of the cation positions are missing. The final parameters for the structure of $NaCsMnTe_2$, which represents a new structure type, are listed in the last column of Table 1 and in Table 8 [35].

3 Results and discussion

3.1 The pure sodium tellurido manganates $Na_2Mn_2Te_3$ and $Na_2Mn_3Te_4$

The two new pure sodium tellurido manganates(II) $Na_2Mn_2Te_3$ and $Na_2Mn_3Te_4$ were obtained in the form of dark-red platelike crystals from melts of the three elements Na, Mn and Te or alternatively from Na, MnTe and Te. $Na_2Mn_3Te_4$ is formed only at maximum temperatures above 700°C. Samples of the target or closely related compositions heated to 600°C yielded the known mixed-valent phase $Na_3Mn_4Te_6$ [25] instead. Further details of the synthesis of the two sodium compounds are collected in the Experimental section.

$Na_2Mn_2Te_3$ crystallizes in the monoclinic space group *C*2/*c* and is isotypic to the analogous sulfido manganate $Na_2Mn_2S_3$ obtained (from sodium carbonate, sulfur and manganese), characterized and described by Klepp et al. as early as 1983 [16]. The isotypic selenido manganate $Na_2Mn_2Se_3$ [17] was obtained from Na, MnSe and Se at a maximum temperature of 850°C by Kim and Hughbanks also already 20 years ago [17]. Further compounds forming this structure type are not known. Different views of the crystal structure of $Na_2Mn_2Te_3$ are shown in Fig. 1.

The layered tellurido manganate anion contains two crystallographically different manganese and three tellurium atoms, all at general Wyckoff positions 8*f* (Table 2). The Te atoms form undulated hexagonal close packed layers (3^6 nets after *Schläfli*) which are running perpendicular to (100) (green nets at the right hand side of the structure drawing in Fig. 1a and b). The sheets are stacked in a hexagonal close packed (h.c.p.; |:AB:|) sequence. Between each second layer, ⅔ of the tetrahedral voids are occupied by Mn^{2+} cations resulting in layers $[Mn_2Te_3]$ of edge and vertex-sharing $[MnTe_4]$ tetrahedra. The occupation of the tetrahedral interstices results in ribbons of equally oriented pairs of tetrahedra (cf. gray bars with arrows in Fig. 1c). The chalcogenido manganate layers finally consist of units of four edge-sharing tetrahedra (blue dotted ellipse in Fig. 1c), which are further connected *via* the μ_3-Te(1) ligands. The common edges within the tetramers $[Mn_4Te(2,3)_4Te(1)_{6/3}]$ are formed by Te(2) and Te(3). The shortest Mn–Mn contacts are lying within this tetramer and are 329.0 [Mn(1)–Mn(2)] and 323.9 pm [Mn(1)–Mn(1)] long. The Mn–Te distances (labeled **a**–**h**) in the tellurido manganate sheets are with 269.6–279.2 pm in the expected range (Table 3). They are shorter than the sum of *Shannon*s radii (287 pm, [39]), but similar to the values found in other tellurido manganates(II), like e.g. in the ortho salts A_6MnTe_4 (275–282 pm, [13, 15]). The sodium cations occupy two special positions 4*e* [site symmetry 2; Na(1) and Na(2)] and one general position [Na(3)]. The Na^+ cations at C_2 symmetric positions occupy (overall ⅔) of the octahedral voids in the interstitial layers between the tellurido manganate sheets. Similar to the Mn centered tetrahedra, $[Na(1,2)Te_6]$ pairs of octahedra form ribbons, which are arranged – under the exclusion of face-sharing – between the ribbons of $[MnTe_4]$ tetrahedra of the adjacent layers. The Na–Te distances within these octahedra are 320–335 pm (Table 3). A separated Na(1) octahedral coordination polyhedron is shown at the right hand side of in Fig. 1a and b. The Na(3) cations are located within the (expanded) Te_3-rings of the tellurium sheets and thus exhibit a five-fold coordination by Te^{2-}, with Na–Te distances of 304–354 pm (cf. the second isolated polyhedron in Fig. 1a and b).

Even though the structure of the long-known compound $Na_3Mn_4Te_6$ shows some similarities with the new phase described above (monoclinic *C* lattice, h.c.p. substructure of Te, sheets of vertex- and edge-sharing $[MnTe_4]$ tetrahedra), the connection of the $[MnTe_4]$ tetrahedra within the sheets is fundamentally different. The two similar-looking compounds $Na_2Mn_2Te_3$ and $Na_3Mn_4Te_6$ show no crystallographic relation (cf. the discussion below) and are thus also not convertible by e.g. an electrochemical redox-induced Na^+ exchange.

The monoclinic crystal structure of the second pure sodium title compound $Na_2Mn_3Te_4$ [28], which is isotypic to the very recently reported selenido analog [18], contains one Na, two Mn and two Te positions (Table 4). Similar to $Na_2Mn_2Te_3$, the structure exhibits tellurido manganate sheets, but in this case Mn(II) is both tetrahedrally and octahedrally coordinated, though it should be pointed out that the latter bonding situation is very rare in alkali sulfido/selenido/tellurido manganates. The Mn(1) atoms at the unit cell origin (2*a*, point group symmetry 2/*m*) are these octahedrally coordinated Mn^{2+} cations ($[Mn(1)Te(1)_{4/4}Te(2)_{2/3}]$, blue polyhedra in Fig. 2). The $[Mn(1)Te_6]$ octahedra are connected *via* opposite edges to form chains running along the *b* axis of the monoclinic cell. As expected, the Mn–Te bond lengths are with 293.3 (**a**) and 325.7 pm (**b**, Table 4) significantly larger than inside the $[Mn^{II}Te_4]$ tetrahedra. However, as illustrated by the 99% ellipsoids of the refinement in the centrosymmetric space group *C*2/*m* [Mn(1) at 0,0,0, cf. Experimental section for details of the refinements] and the difference electron density map (Fig. 2a and b) Mn(1) is evidently slightly disordered around the 2*a* site (Δ≈25 pm), leading to a distortion of the octahedra towards a square pyramid and to two different distances **b** to the Te(2) octahedra tips of ≈300 and 350 pm. The very same situation has been described for the isotypic selenido compound $Na_2Mn_3Se_4$ [18]. The second type of Mn(II) cations in the structure of $Na_2Mn_3Te_4$ [Mn(2), Wyckoff site 4*i*, *m* symmetry] are tetrahedrally coordinated by four Te^{2-} anions ($[MnTe(1)_{2/4}Te(2)_{2/3}]$, gray polyhedra in Fig. 2), whereby two tetrahedra form dinuclear units sharing a common edge. These dimers are again connected *via* four common corners to form strands, which are again running along *b*. The Mn(2)–Te bond lengths are again in the range common for tetrahedral building blocks (270.8–279.2 pm, Table 5). The ribbons of octahedra and tetrahedra are fused and form puckered layers $[Mn_3Te_4]^{2-}$ in the *b*–*c* plane, which are |:AB:| stacked along [100]. Between the layers, Na^+ cations (Wyckoff position 4*i*) are interspersed, which exhibit an octahedral coordination with very similar distances like in $Na_2Mn_2Te_3$ (d_{Na-Te} = 317.3–356.9 pm, yellow polyhedra). In contrast to the simple Te^{2-} layers found in $Na_2Mn_2Te_3$ [3^6 nets, (defect) $CaAl_2Si_2$-type] and the tellurido compounds with the larger *A* cations [4^4 nets, $ThCr_2Si_2$-type, see below], the Te atoms in $Na_2Mn_3Te_4$ form $3^3 \cdot 4^2$ nets: the planar nets running in the *a*–*c* plane at *y* = ¼ and ¾ are marked by red arrows in Fig. 2c; the second set of slightly puckered similar nets along the diagonal are marked by blue arrows. The four-membered

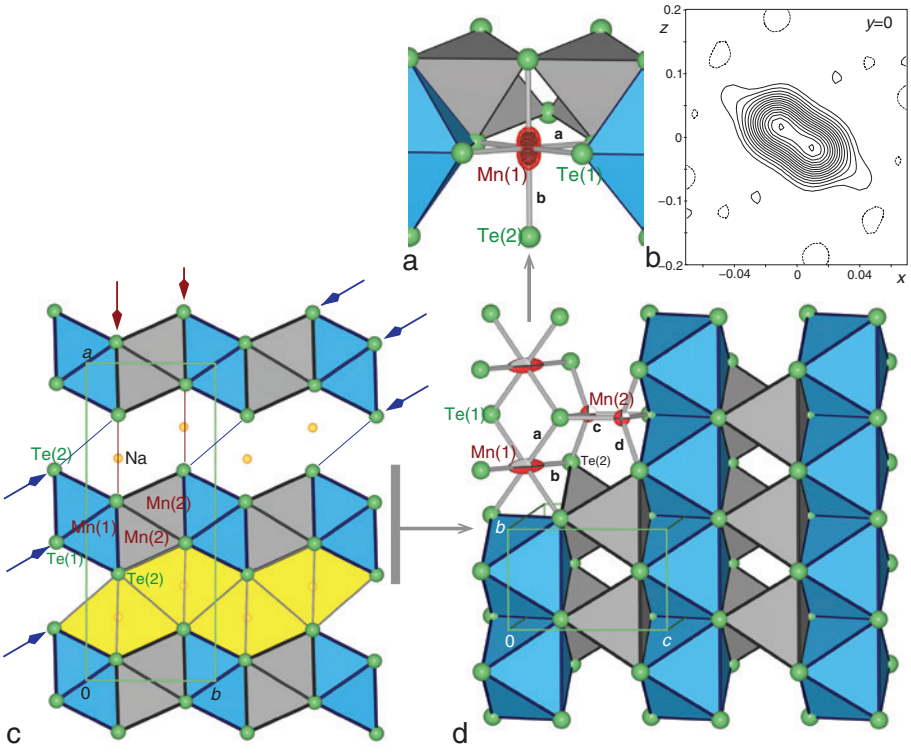

Fig. 2: Crystal structure of $Na_2Mn_3Te_4$. a/b: details of the surrounding of Mn(1), with the difference electron density around Mn(1) plotted at a level of 3 (solid) and 15 (red net) $e^- \times 10^{-6}$ pm^{-3} (a) and difference electron density map with isolines of 1 $e^- \times 10^{-6}$ pm^{-3} (b). (c) Projection of the structure along *c*; (d) perspective view of the tellurido manganate sheet, with Mn ellipsoids at a level of 99% (cf. Fig. 1 for a detailed legend and Table 5 for interatomic distances).

Table 5: Selected interatomic distances (pm) and coordination numbers in the crystal structure of $Na_2Mn_3Te_4$.

Atoms		Distance	Label	Mult.	CN	Atoms		Distance	Label	Mult.	CN	Atoms		Distance	Label	Mult.	CN
Na	– Te(1)	317.3(2)		2×		Mn(1)	– Te(1)	293.3(1)	**a**	4×		Mn(2)	– Te(2)	272.3(1)	**c**	2×	
	– Te(2)	320.7(2)		2×			– Te(2)	325.7(1)	**b**	2×	6		– Te(1)	272.3(1)	**d**		
	– Te(2)	346.1(3)											– Te(1)	272.9(1)	**e**		4
	– Te(2)	356.9(3)			6								– Mn(2)	330.7(1)	**u**	1×	
Te(1)	– Mn(2)	272.3(1)	**c**			Te(2)	– Mn(2)	272.3(1)	**c**	2×							
	– Mn(2)	272.9(1)	**e**				– Na	320.7(2)		2×							
	– Mn(1)	293.3(1)	**a**	2×			– Mn(1)	325.7(1)	**b**								
	– Na	317.3(2)		2×	4+2		– Na	346.1(3)									
							– Na	356.9(3)			3+4						

rings of these tellurium nets coincide with the 'bases' of the [Mn(1)Te_6] (blue layers) and the [$NaTe_6$] octahedra (red layers).

Even though the structure type of the two compounds $Na_2Mn_3Se_4$ and $Na_2Mn_3Te_4$ [18] is singular, it is however closely related to the isopointal sodium sulfido metallate $Na_2Cu_2ZrS_4$ [40]: in the latter compound, the chalcogen packing as well as the arrangements of the [ZrS_6] and the [NaS_6] octahedra are similar. The only difference is the connection of the [$Cu^{II}S_4$] tetrahedra, which form *zweier* single zig-zag chains along *b* sharing two adjacent edges, while $Na_2Mn_3Se_4$ and $Na_2Mn_3Te_4$ exhibit *einer* double chains of [Mn_2Q_6] dinuclear units.

3.2 Mixed tellurido manganates Na_2AMnTe_3 (*A* = K, Rb)

Despite its very simple overall composition A_3MnTe_3, which suggests the presence of Mn(III), the mixed tellurido manganates Na_2AMnTe_3 (*A* = K, Rb) exhibit an unexpectedly complex crystal structure. However, the bonding situation

is closely related to that in the cobaltate Na_3CoS_3 [12], where *Q*–*Q* bonds are present and the metal cation is kept at an oxidation state of +II. For Na_3CoS_3, the polyanions formed are already complex, but the two manganates Na_2AMnTe_3 show an even more diverse structural chemistry. The new chiral orthorhombic structure type (space group $Pmc2_1$) consists of five crystallographically different sodium and two K/Rb cations (Table 6). The anionic building blocks contain four manganese and 10 tellurium sites, which are labelled according to their bonding features. The polyanions are best divided into two different layers coinciding with the mirror planes at $x = ½$ (layers **A**) and $x = 0$ (**B**). The layers consist of chains formed by two crystallographically different Mn(II) cations each.

The layers **A** are formed by chains of $[Mn(1,2)Te_4]$ tetrahedra, alternately connected *via* common edges and corners (Fig. 3a). The chains of layer **A** are running along [001] around $y \approx ½$. Whereas Mn(1) is coordinated by monatomic tellurido ligands Te^{2-} only, the η_1 tellurido ligand bonded to Mn(2) is a ditelluride dumbbell $[Te(21,22)_2]^{2-}$. The chains are composed of vertex-sharing dinuclear units $[Te(2)_{1/2}Te(1)Mn(1)Te(12)_2Mn(2)(Te_2)Te(2)_{1/2}]$, which themselves consist of the edge-sharing tetrahedra $[Mn(1)Te(1)Te_{3/2}]$ and $[Mn(2)(Te)_2Te_{3/2}]$. The overall formula of the chains within the layer **A** is thus $^1_\infty[Mn_2Te_6]^{6-}$ and therewith meets the composition of the whole compound. The sodium cations Na(1), which exhibit a trigonal bipyramidal coordination, are located at the same mirror plane.

The second mirror plane (at $x = 0$, layers **B**, Fig. 3b) again contains angulated chains of $[MnTe_4]$ tetrahedra also running along the *c* axis. In this case, the tetrahedra are connected *via* edges exclusively; their overall formula is thus $^1_\infty[MnTe_{4/2}]^{2-}$. These chains around $y \approx 0$ are staggered against the chains of the adjacent layers **A**. The mirror planes **B** are additionally occupied by $[Te(31,32)_2]^{2-}$ dumbbells, which are not connected to manganese atoms, but fill the space between the $[MnTe_{4/2}]^{2-}$ chains. Due to the ratio of these $[Te_2]^{2-}$ dumbbells and the $[MnTe_{4/2}]^{2-}$ tetrahedra of 1:2 the total composition and charge of this layer **B** $[Mn_2Te_4]^{4-}[Te_2]^{2-} = [Mn_2Te_6]^{6-}$ is again similar to that of the overall formula. The cations Na(2) are also located at this mirror plane and are stuffed between the ditelluride dumbbells and the Te(¾) atoms of the chains. They show a pentagonal-bipyramidal 7-fold coordination by Te atoms (transparent yellow polyhedron in Fig. 3d).

The remaining alkali cations (the three sodium Na(3), Na(4), Na(5) and the two Rb/Cs cations) are located close to $x = ¼$ (and ¾) and thus form only very slightly puckered nets with the *Schläfli* symbol 3.5.3.5. (Na nodes) + 3^2.5.3.5. (Rb nodes) (3:2). The five-membered rings of this net of cations are centered by the Te(12) and Te(34) atoms

Table 6: Atomic coordinates and equivalent isotropic displacement parameters/pm² for the crystal structures of Na_2AMnTe_3 (*A* = K, Rb).

Atoms	Wyckoff position	*x*		*y*		*z*		U_{eq}	
		A = K	*A* = Rb	*A* = K	*A* = Rb	*A* = K	*A* = Rb	*A* = K	*A* = Rb
Na(1)	2*b*	1/2	1/2	0.0790(5)	0.1070(3)	0.3282(7)	0.3230(3)	337(14)	254(7)
Na(2)	2*a*	0	0	0.4296(5)	0.4320(2)	−0.0007(6)	−0.0037(3)	307(13)	207(6)
Na(3)	4*c*	0.2685(4)	0.26977(17)	0.0061(5)	0.00606(15)	0.5817(5)	0.58479(17)	375(10)	146(4)
Na(4)	4*c*	0.2802(5)	0.27845(17)	0.5078(4)	0.50723(16)	0.2507(4)	0.24983(16)	340(9)	137(3)
Na(5)	4*c*	0.2155(6)	0.21766(19)	0.2545(4)	0.25215(14)	0.1721(5)	0.17129(19)	455(13)	163(4)
A(1)	4*c*	0.2220(3)	0.21975(4)	0.29934(19)	0.30032(3)	0.4955(3)	0.49539(4)	382(5)	101.7(7)
A(2)	4*c*	0.2586(3)	0.26218(4)	0.19882(19)	0.19831(3)	0.8367(3)	0.83540(4)	399(5)	114.4(7)
Mn(1)	2*b*	1/2	1/2	0.32499(17)	0.32787(7)	0.0784(2)	0.07895(8)	243(4)	90(2)
Mn(2)	2*b*	1/2	1/2	0.45944(15)	0.46297(6)	0.4820(2)	0.48216(8)	247(4)	91(2)
Mn(3)	2*a*	0	0	0.03978(18)	0.03708(7)	0.45439(19)	0.45517(8)	248(4)	97(2)
Mn(4)	2*a*	0	0	0.04119(17)	0.04325(7)	0.20812(19)	0.21011(8)	239(4)	92(2)
Te(1)	2*b*	1/2	1/2	0.12935(7)	0.13242(3)	0.03820(10)	0.05131(3)	289(2)	108.8(8)
Te(2)	2*b*	1/2	1/2	0.34101(8)	0.34731(3)	0.30507(8)	0.30426(3)	274(2)	96.6(8)
Te(12)	4*c*	0.29425(6)	0.29096(2)	0.42356(4)	0.42324(2)	0.00159(6)	0.00155(2)	242.4(13)	81.8(5)
Te(21)	2*b*	1/2	1/2	0.65730(8)	0.65474(3)	0.17100(9)	0.16930(3)	276(2)	88.5(7)
Te(22)	2*b*	1/2	1/2	0.14231(8)	0.14828(3)	0.61941(9)	0.61086(3)	299(2)	108.0(8)
Te(3)	2*a*	0	0	0.15089(8)	0.14545(3)	0.63706(8)	0.63849(3)	269(2)	88.3(7)
Te(4)	2*a*	0	0	0.15388(7)	0.15407(3)	0.02502(8)	0.02785(3)	258(2)	89.7(7)
Te(31)	2*a*	0	0	0.39414(8)	0.39761(3)	0.28947(9)	0.28281(3)	285(2)	104.8(8)
Te(32)	2*a*	0	0	0.59469(8)	0.59711(3)	0.22087(9)	0.22001(3)	287(2)	101.3(8)
Te(34)	4*c*	0.20575(6)	0.21003(2)	0.07459(5)	0.07380(2)	0.33184(6)	0.33329(2)	267.1(13)	93.3(5)

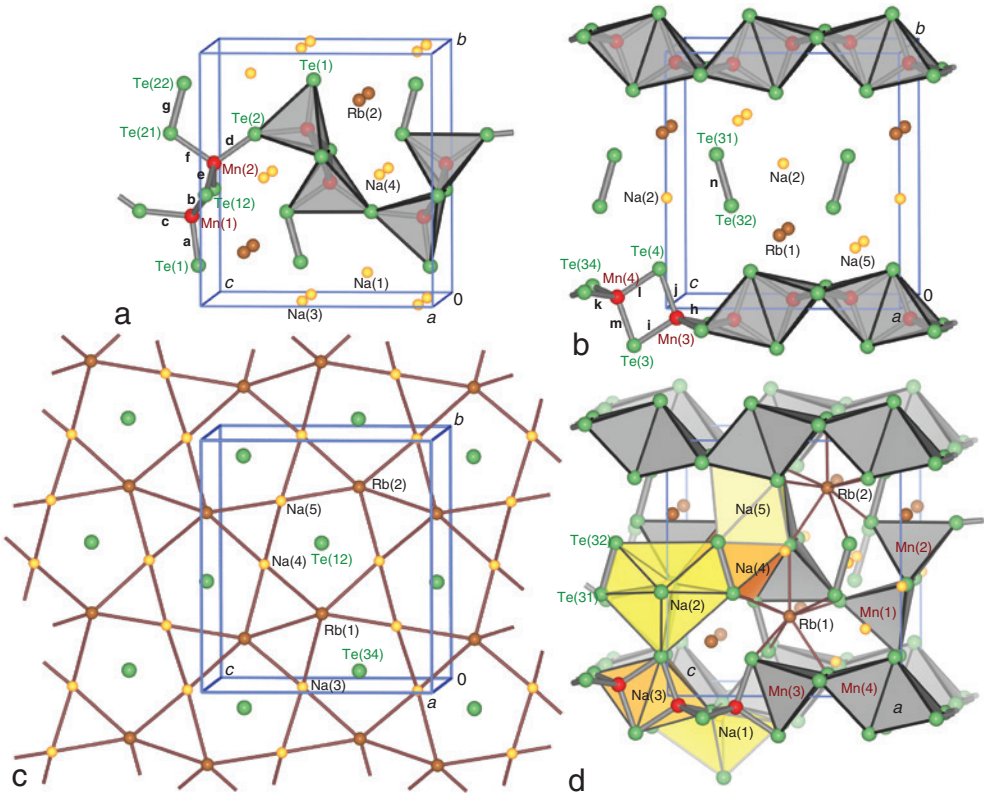

Fig. 3: Crystal structure of Na_2AMnTe_3. (a) Chains $[Mn(1,2)_2Te_6]^{6-}$ (layer **A**) around $x \approx ½$. (b) Chains $[Mn(3,4)_2Te_4]^{4-}$ and $[Te_2]^{2-}$ dumbbells (layer **B**) around $x \approx 0$ and 1. (c) Cation nets [Rb and Na(3) to Na(5)] at $x \approx ¼$ and ¾. (d) Perspective view of the unit cell together with all cation coordination spheres (Rb, brown sticks) and polyhedra (Na, yellowish polyhedra; cf. Table 7 for interatomic distances and their labels).

forming those common edges of the $[MnTe_4]$ tetrahedra, which are oriented perpendicular to the mirror planes. The three sodium cations exhibit distorted octahedral coordination spheres (yellow polyhedra in Fig. 3d) with Na–Te distances in the range 312–386 pm (Table 7). As expected from the increased ionic radii, the heavier alkali cations K^+ and Rb^+ are coordinated by eight [A(2): 7 + 1] tellurium atoms with larger distances of minimum 356 pm. The respective coordination spheres are shown by thin brown 'bonds' in Fig. 3d.

The Mn–Te bond lengths within the $[MnTe_4]$ tetrahedra are again in the usual range between 269 and 282 pm. Compared to the pure Na compounds above, these Te-richer compounds exhibit μ_1- and μ_2-Te^{2-} ligands only and the tetrahedra are less connected with each other. In addition to the one or two Mn^{2+} cations, five to seven A^+ cations round out the tellurium coordination spheres. The Te(22) and Te(32) atoms, which are not connected to manganese, show a 1 Te + 8 A coordination sphere (Table 7), which is likewise observed in binary alkali (poly)tellurides (cf. discussions in [41, 42]). The Te–Te bonds within the dumbbells amount to 276/278 pm for the $[Te_2]$ ligands and 280/284 pm for the 'free' ditelluride anions. These slightly decreased bond lengths of bonded dichalcogenid anions are similarly observed for other dichalcogenido metallates (like e.g. Na_3CoS_3 [12]) and are sufficiently discussed in the literature [43, 44].

3.3 $NaCsMnTe_2$

$NaCsMnTe_2$ crystallizes in a new, very simple, but nevertheless new, orthorhombic structure type (space group *Cccm*). The crystal parameters are collected in the last column of Table 1 and in Table 8, interatomic distances can be found in Table 9.

The compound exhibits the largest differences in the size of the two alkali cations, Na^+ and Cs^+. Consequently, the cations are again fully ordered at two crystallographically different positions with very diverse coordination numbers of four (tetrahedra, for Na^+, transparent yellow polyhedra in Fig. 4) and eight (cubes, for Cs^+). The tellurido manganate(II) polyanions are linear chains of edge-sharing tetrahedra $[MnTe_{4/2}]$, which are running along the

Table 7: Selected interatomic distances (pm) in the crystal structure of Na_2AMnTe_3 (A = K, Rb).

Atoms		Distance		Label	Freq.	CN	Atoms		Distance		Label	Freq.	CN	Atoms		Distance		CN
		A=K	*A*=Rb						*A*=K	*A*=Rb						*A*=K	*A*=Rb	
Na(1)	– Te(34)	314.8(1)	312.1(1)		2×		Na(2)	– Te(12)	314.9(1)	310.0(1)		2×		Na(3)	– Te(22)	312.0(5)	313.0(2)	
	– Te(2)	355.0(7)	325.3(4)					– Te(32)	346.5(8)	344.0(3)					– Te(1)	312.6(5)	311.0(2)	
	– Te(1)	365.6(9)	337.8(3)					– Te(31)	352.4(7)	350.2(3)					– Te(34)	330.0(7)	330.4(2)	
	– Te(22)	370.8(9)	360.4(3)			5		– Te(32)	353.6(8)	355.4(3)					– Te(34)	335.2(7)	331.9(2)	
								– Te(31)	362.7(8)	357.5(3)			6		– Te(3)	354.1(5)	349.7(2)	
															– Te(4)	366.1(5)	366.3(2)	6
Na(4)	– Te(32)	324.1(5)	322.4(2)				Na(5)	– Te(34)	313.5(5)	313.4(2)								
	– Te(12)	324.6(5)	325.5(2)					– Te(12)	322.2(5)	321.8(2)								
	– Te(21)	325.2(5)	324.4(2)					– Te(4)	323.8(6)	320.4(2)								
	– Te(12)	329.3(5)	327.7(2)					– Te(31)	331.4(6)	333.6(2)								
	– Te(2)	332.4(5)	326.8(2)					– Te(2)	365.2(6)	365.9(2)								
	– Te(31)	340.2(5)	333.8(2)			6		– Te(1)	385.6(1)	372.1(2)			6					
A(1)	– Te(3)	356.8(3)	360.3(1)				*A*(2)	– Te(4)	366.9(3)	371.6(1)								
	– Te(34)	365.4(3)	365.9(1)					– Te(12)	367.7(3)	368.0(1)								
	– Te(31)	371.4(3)	375.6(1)					– Te(1)	371.2(3)	378.6(1)								
	– Te(21)	373.0(3)	372.7(1)					– Te(34)	373.5(3)	371.7(1)								
	– Te(12)	382.1(3)	381.0(1)					– Te(3)	376.7(3)	377.2(1)								
	– Te(2)	383.8(3)	385.9(1)					– Te(22)	380.8(3)	381.8(1)								
	– Te(32)	393.4(3)	388.7(1)					– Te(21)	382.9(3)	381.7(1)								
	– Te(22)	396.2(3)	389.3(1)			8		– Te(32)	418.1(3)	417.8(1)			8					
Layer A							**Layer B**											
Mn(1)	– Te(1)	268.8(3)	266.2(1)	**a**			Mn(3)	– Te(34)	271.5(2)	274.2(1)	**h**	2×						
	– Te(12)	274.2(2)	274.3(1)	**b**	2×			– Te(3)	271.5(3)	269.9(1)	**i**							
	– Te(2)	281.6(3)	279.9(1)	**c**		4		– Te(4)	275.7(3)	273.4(1)	**j**		4					
	– Mn(2)	314.6(3)	306.9(1)					– Mn(4)	305.1(3)	303.2(1)	**v**							
Mn(2)	– Te(2)	271.3(2)	269.9(1)	**d**			Mn(4)	– Te(34)	272.0(2)	273.7(1)	**k**	2×						
	– Te(12)	272.0(1)	271.5(1)	**e**	2×			– Te(4)	273.1(3)	270.6(1)	**l**							
	– Te(21)	282.2(3)	280.8(1)	**f**		4		– Te(3)	273.9(3)	269.8(1)	**m**		4					
	– Mn(1)	314.6(3)	306.8(1)	**u**				– Mn(3)	305.1(3)	303.2(1)	**v**							
Te(1)	– Mn(1)	268.8(3)	266.2(1)	**a**			Te(3)	– Mn(3)	271.5(3)	269.9(1)	**i**							
	– Na(3)	312.6(5)	311.0(2)		2×			– Mn(4)	273.9(3)	269.8(1)	**m**							
	– Na(1)	365.6(9)	337.8(3)					– Na(3)	354.1(5)	349.7(2)		2×						
	– *A*(2)	371.2(3)	378.6(1)					– *A*(1)	356.8(3)	360.3(1)		2×						
	– Na(5)	385.6(1)	372.1(2)			1+5		– *A*(2)	376.7(3)	377.2(1)		2×	2+6					
Te(2)	– Mn(2)	271.3(2)	269.9(1)	**d**			Te(4)	– Mn(4)	273.1(3)	270.6(1)	**l**							
	– Mn(1)	268.8(3)	266.2(1)	**a**				– Mn(3)	275.7(3)	273.4(1)	**j**							
	– Na(4)	332.4(5)	326.8(2)		2×			– Na(5)	323.8(6)	320.4(2)								
	– Na(1)	355.0(7)	325.3(4)					– Na(3)	366.1(5)	366.3(2)		2×						
	– Na(5)	365.2(6)	365.9(2)		2×			– *A*(2)	366.9(3)	371.6(1)		2×	2+5					
	– *A*(1)	383.8(3)	385.9(1)		2×	2+7												
							Te(34)	– Mn(3)	271.5(2)	274.2(1)	**h**							

Table 7 (continued)

Atoms		Distance		Label	Freq.	CN	Atoms		Distance		Label	Freq.	CN	Atoms		Distance		CN
		A=K	*A*=Rb						*A*=K	*A*=Rb						*A*=K	*A*=Rb	
Te(12)	– Mn(2)	272.0(1)	271.5(1)	**e**				– Mn(4)	272.0(2)	273.7(1)	**k**							
	– Mn(1)	274.2(2)	274.3(1)	**b**				– Na(5)	313.5(5)	313.4(2)								
	– Na(2)	314.9(1)	310.0(1)					– Na(1)	314.8(1)	312.1(1)								
	– Na(5)	322.2(5)	321.8(2)					– Na(3)	330.0(7)	330.4(2)								
	– Na(4)	324.6(5)	325.5(2)					– Na(3)	335.2(7)	331.9(2)								
	– Na(4)	329.3(5)	327.7(2)					– *A*(1)	365.4(3)	365.9(1)								
	– *A*(2)	367.7(3)	368.0(1)					– *A*(2)	373.5(3)	371.7(1)			2+6					
	– *A*(1)	382.1(3)	381.0(1)			2+6												
							Te(31)	– Te(32)	283.8(2)	280.4(1)	**n**							
Te(21)	– Te(22)	278.0(2)	275.7(1)	**g**				– Na(5)	331.4(6)	333.6(2)		2×						
	– Mn(2)	282.2(3)	280.8(1)	**f**				– Na(4)	340.2(5)	333.8(2)		2×						
	– Na(4)	325.2(5)	324.4(2)		2×			– Na(2)	352.4(7)	350.2(3)								
	– *A*(1)	373.0(3)	372.7(1)		2×			– Na(2)	362.7(8)	357.5(3)								
	– *A*(2)	382.9(3)	381.7(1)		2×	1+1+6		– *A*(1)	371.4(3)	375.6(1)		2×	1+7					
Te(22)	– Te(21)	278.0(2)	275.7(1)	**g**			Te(32)	– Te(31)	283.8(2)	280.4(1)	**n**							
	– Na(3)	312.0(5)	313.0(2)		2×			– Na(4)	324.1(5)	322.4(2)		2×						
	– Na(1)	370.8(9)	360.4(3)		2×			– Na(2)	346.5(8)	344.0(3)		2×						
	– *A*(2)	380.8(3)	381.8(1)		2×			– *A*(1)	393.4(3)	388.7(1)		2×						
	– *A*(1)	396.2(3)	389.3(1)		2×	1+8		– *A*(2)	418.1(3)	417.8(1)		2×	1+8					

Table 8: Atomic coordinates and equivalent isotropic displacement parameters/pm² for the crystal structure of $NaCsMnTe_2$.

Atoms	Wyckoff position	*x*	*y*	*z*	U_{eq}
Na	4*a*	0	0	1/4	110(2)
Cs	4*e*	1/4	1/4	0	133.4(5)
Mn	4*b*	0	1/2	1/4	77.1(9)
Te	8*l*	0.21609(2)	0.60639(2)	0	76.8(4)

Table 9: Selected interatomic distances (pm) in the crystal structure of $NaCsMnTe_2$.

Atoms		Distance	Label	Freq.	CN
Na	– Te	305.229(13)		4×	4
Cs	– Te	391.65(2)		2×	
	– Te	399.533(12)		4×	
	– Te	431.36(2)		2×	8
Mn	– Te	277.173(12)	**a**	4×	4
Te	– Mn	277.174(12)		2×	
	– Na	305.232(13)		2×	
	– Cs	391.65(2)			
	– Cs	399.531(12)		2×	
	– Cs	431.36(2)			2+(2+4)

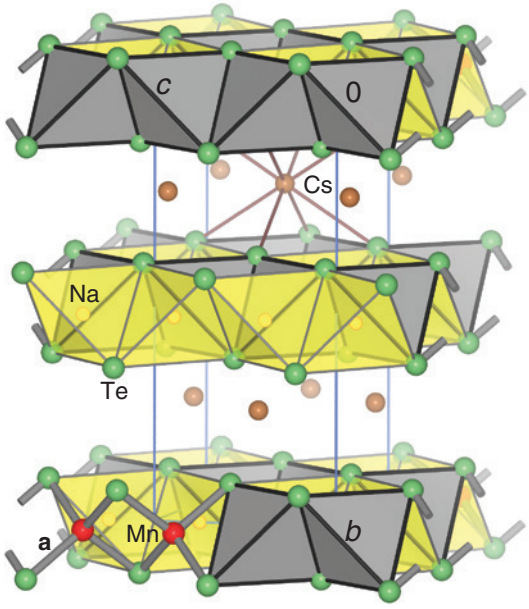

Fig. 4: Crystal structure of $NaCsMnTe_2$ (cf. Table 9 for interatomic distances; caption of Fig. 1).

c axis. The Mn–Te distance of 277.2 pm is again approx. 10 pm shorter than the sum of *Shannon*s radii (287 pm, [39]), but very similar to the bond lengths in the chains of the pure alkali compounds $(K/Rb/Cs)_2MnTe_2$ forming the K_2ZnO_2-type structure (e.g. Cs_2MnTe_2: d_{Mn-Te} = 277.3 pm [8]). The bond angles Te–Mn–Te within the tetrahedra are 106.4–114.5° and the polyhedra are therewith slightly stretched along the chain direction. The $[NaTe_{4/2}]$ tetrahedra are connected among each other in a similar manner, the Na–Te distance of 305.2 pm is also somewhat decreased with respect to the sum of the *Shannon* radii of 320 pm. Similar short values can be found e.g. for Na(3) with CN = 5 in $Na_2Mn_2Te_3$ (303.7 pm, Table 2), whereas the Na–Te distances within octahedra are commonly somewhat larger (e.g. $Na_2Mn_2Te_3$: d_{Na-Te} = 320–334 pm). Both chains of tetrahedra share the tellurium atoms and are thus connected to PbO-like layers $[NaMnTe_2]$, which are also the building blocks in the prominent $ThCr_2Si_2$-type iron arsenido and chalcogenido superconductors and generally in many alkali-poorer chalcogenido-metallates with larger counter-cations K^+ to Cs^+. Analogously, the larger cation Cs^+ in $NaCsMnTe_2$ occupies the alkali (Th in the aristotype) position between the layers. The pseudo-tetragonal orthorhombic unit cell, in which the *a* and the *c* axis are of comparable lengths, is a consequence of this structure relation. Not surprisingly, the new structure type can be crystallographically derived by a group subgroup relation [45–48] from the $BaAl_4/ThCr_2Si_2$-type by firstly applying a *t*2 symmetry reduction from the space group *I*4/*mmm* of the aristotype to *Fmmm* (basis change: $\mathbf{a}' = \mathbf{a} - \mathbf{b}$, $\mathbf{b}' = \mathbf{a} + \mathbf{b}$). Secondly, a *k*2 symmetry reduction leads directly to the space group *Cccm* of $NaCsMnTe_2$ (cf. Fig. 5). Thereby the Ba/Th Wyckoff position 2*a* transforms to 4*e* (Cs), the 4*d* site [Cr/Al(1)/*M* in the chalcogenido metallates AM_2Q_2] splits into 4*a* (Na) and 4*b* (Mn), again without any free positional parameter. The 4*e* position of the aristotype (0,0,*z*) with a free *z* parameter and point group 4*mm* is transformed to the 8*l* position of the Te anions (~¼, ~¼ + *z*, 0; cf. Table 8).

For the closely related Li/K sulfido manganate $KLiMnS_2$, Bronger et al. reported the statistic occupation of Li^+ and Mn^{2+} at the Cr sites of the aristotype [49].

3.4 Classification of the title compounds within the family of alkali chalcogenido manganates

The five title compounds can be classified within the families of known alkali chalcogenido (excluding oxygen) manganates(II) and (III). To that, Table 10 contains the basic structure data of all compounds reported in the literature. The manganates can obviously be categorized according to the connectivity of the $[MnQ_4]$ tetrahedra into (i) 'ortho' salts containing isolated tetrahedra,

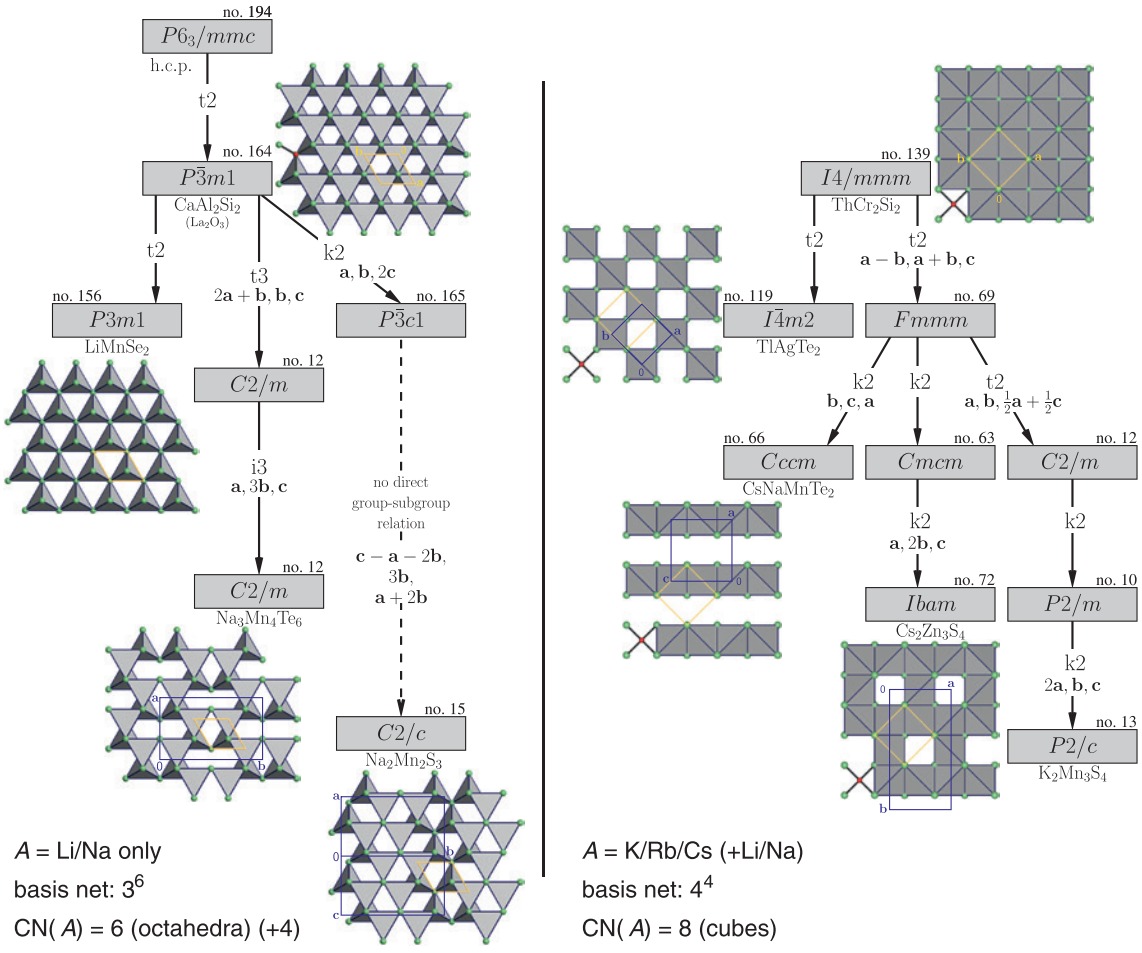

Fig. 5: Structure relations (if possible, with a crystallographic group-subgroup relation) of Li/Na chalcogenido manganates basing on a hexagonal close packing of Q^{2-} (left, $CaAl_2Si_2$-aristotype) and (right) K/Rb/Cs-containing compounds related to the $ThCr_2Si_2$-aristotype (see text).

(ii) 'ino' compounds containing chains of edge-connected tetrahedra $^1_\infty[MnQ_{4/2}]$ and (iii) finally several types of 'phyllo' manganates of different types with layered manganate polyanions. The two new isotypic 'phyllo' compounds $Na_2Mn_3Se_4$ [18] and $Na_2Mn_3Te_4$ are the only examples of S/Se/Te manganates containing (besides a tetrahedral) an octahedrally coordinated Mn(II). Despite this general difference, the structure can be related to the remaining layered Li/Na manganates, if the compounds are categorized according to their basic *Q* packing (see below).

(i) For the lighter alkali elements sodium and potassium, the *ortho* metallate salts $A_6M^{II}Q_4$ of the 3*d* elements Mn and Co, which strongly prefer the oxidation state +II in S, Se and Te compounds, are long-known [13, 14, 53–56]. All compounds of this composition form the Na_6ZnO_4-type structure. While lithium salts of this type are missing, the structure family has recently been extended to the respective manganates(II) of rubidium and cesium, which are indeed isotypic to the Na/K salts [15]. Attempts to prepare other Rb/Cs metallate(II) salts of this type (i.e. Co, Zn, Cd compounds) are subject of ongoing work. The Na_6ZnO_4-type structure exhibits a h.c.p. arrangement of the chalcogenid ions and is crystallographically connected by a group-subgroup relation with the Mg-type (h.c.p.) structure (cf. discussion and *Bärnighausen* symmetry tree in [15]). In contrast to the less *A*-richer 'ino' and 'phyllo' manganates discussed below, also the larger Rb^+ and Cs^+ cations occupy (distorted) octahedral and even tetrahedral voids in the chalcogenide close packing.

For some 'ino' and all 'phyllo' manganates(II) and (III), the basic chalcogenide packing is determined by the different coordination spheres of the *A* cations: the pure Li and Na salts can be derived from a hexagonal close packing of Q^{2-} (3^6 nets), in which all cations (A^+ and Mn^{2+})

Table 10: Summary of known alkali chalcogenido manganates.

Type	OS of Mn	General composition	Individual compound(s)	Reference	Structure type	Space group	Mn–*Q* distance/pm (CN)[b]	Building blocks, comments, etc.
Ortho-	2	A_6MnQ_4	$(Na/K)_6MnS_4$	[13, 14]	Na_6ZnO_4	$P6_3mc$	242.4–246.7	Isolated tetrahedra $[MnQ_4]$
			$(Na/K)_6MnSe_4$	[13]	Na_6ZnO_4	$P6_3mc$	254.5–259.2	
			$(Na/K)_6MnTe_4$	[13]	Na_6ZnO_4	$P6_3mc$	275.4–278.6	
			$(Rb/Cs)_6MnS_4$	[15]	Na_6ZnO_4	$P6_3mc$	248.7–250.7	
			$(Rb/Cs)_6MnSe_4$	[15]	Na_6ZnO_4	$P6_3mc$	260.7–263.0	
			$(Rb/Cs)_6MnTe_4$	[15]	Na_6ZnO_4	$P6_3mc$	280.0–282.4	
Ino-	2	A_2MnQ_2	$(K/Rb/Cs)_2MnS_2$	[8]	K_2ZnO_2	*Ibam*	243.5–247.4	Linear chains of $[MnQ_{4/2}]$ tetrahedra
			$(K/Rb/Cs)_2MnSe_2$	[8]	K_2ZnO_2	*Ibam*	256.2–257.6	
			$(K/Rb/Cs)_2MnTe_2$	[8]	K_2ZnO_2	*Ibam*	275.2–277.3	
			$NaCsMnTe_2$	[a]	New	*Cccm*	cf. Table 9	
			$LiNaMnS_2$	[23]	$CaAl_2Si_2$	$P\bar{3}m1$	(244.3–247.8)	Li/Mn statistically distributed
			$Li(K/Rb/Cs)MnS_2$	[49]	$ThCr_2Si_2$	$I4/mmm$	(243.9–252.7)	
		A_3MnQ_3	$Na_2(K/Rb)MnTe_3$	[a]	New	$Pmc2_1$	cf. Table 7	Te–Te bonds
Phyllo-	2	$A_2Mn_2Q_3$	$Na_2Mn_2S_3$	[16]	$Na_2Mn_2S_3$	$C2/c$	239.3–246.5	Sheets of edge-sharing tetrahedra
			$Na_2Mn_2Se_3$	[17]	$Na_2Mn_2S_3$	$C2/c$	251.9–260.2	
			$Na_2Mn_2Te_3$	[a]	$Na_2Mn_2S_3$	$C2/c$	269.6–279.2	
		$A_2Mn_3Q_4$	$Na_2Mn_3Se_4$	[18]	$Na_2Mn_3Te_4$	$C2/m$	252.2–254.9(4)	Sheets of $[MnQ_4]$ tetrahedra and $[MnQ_6]$ octahedra
							272.1–296.9(6)	
			$Na_2Mn_3Te_4$	[a], [28]	$Na_2Mn_3Te_4$	$C2/m$	272.3–272.9(4)	
							272.1–296.9(6)	
			$K_2Mn_3S_4$	[19, 20]	Singular	$P2/c$	239.7–245.3	cf. Fig. 2
			$(Rb/Cs)_2Mn_3S_4$	[50–52]	$Cs_2Mn_3S_4$	*Ibam*	241.9–246.0	Defect variants of $ThCr_2Si_2$ type layers
			$(Rb/Cs)_2Mn_3Se_4$	[18, 21]	$Cs_2Mn_3S_4$	*Ibam*	254.1–257.9	
			$(Rb/Cs)_2Mn_3Te_4$	[21]	$Cs_2Mn_3S_4$	*Ibam*	275.1–277.6	
	2.25		$Na_3Mn_4Te_6$	[24]	Singular	$C2/m$	277.0–280.6	Defect variants of the $CaAl_2Si_2$-layers
			$NaMn_{1.56}Te_2$	[24]	$CaAl_2Si_2$	$P\bar{3}m1$	274.9–280.8	
	3	$AMnQ_2$	$(Li/Na)MnSe_2$	[17]	$LiMnSe_2$	$P3m1$	255.5–259.7	Ordered defect variants with $CaAl_2Si_2$ layers
			$(Li/Na)MnTe_2$	[25]	$LiMnSe_2$	$P3m1$	276.8–278.4	
			$(K/Rb/Cs)MnSe_2$	[17]	$TlAgTe_2$	$I\bar{4}m2$	256.9 (A = Rb)	Ordered defect variants with $ThCr_2Si_2$ layers
			$(K/Rb/Cs)MnTe_2$	[24]	$TlAgTe_2$	$I\bar{4}m2$	277.7–278.2	

[a]This work. [b]Distances from derived coordinates in brackets. OS, (averaged) oxidation state.

occupy tetrahedral and/or octahedral voids. Structures belonging to this family are collected in the symmetry tree depicted at the left hand side of Fig. 5. The aristotype for the layered compounds is $CaAl_2Si_2$ (or similarly La_2O_3). All salts containing K, Rb or Cs (optionally together with Li or Na) contain these larger cations in a cubic eight-fold coordination by *Q*. In these cases, the basic chalcogen arrangement corresponds to the nine-fold close packing [49] consisting of 4^4 nets and $ThCr_2Si_2/BaZn_2P_2$ as aristotype (right hand side of Fig. 5).

(ii) Similar to the ortho salts, the sulfido, selenido and tellurido *chain* ('ino') manganates A_2MnQ_2, which are known for the heavier alkali elements K, Rb and Cs only [8], are all isotypic (K_2ZnO_2-type). The orthorhombic structure contains linear chains $^1_\infty[MnQ_{4/2}]$ separated by alkali cations, the latter with a distorted octahedral coordination by the chalcogen atoms. Despite the similar building blocks, *A*/*M* coordinations, unit cell dimensions and the same space group (*Ibam*), the K_2ZnO_2-type is not crystallographically related to the layered compounds of the $ThCr_2Si_2$-aristotype (e.g. $Cs_2Mn_3S_4$-type). In contrast, the new compound $CsNaMnTe_2$, which contains layers $[NaMnTe_2]$ built up of two fused parallel $[NaTe_{4/2}]$ and chains of $[MnTe_{4/2}]$ tetrahedra, can be very simply derived from this aristotype (cf. structure description above and the right hand side symmetry tree in Fig. 5). For the ternary lithium K/Rb/Cs compounds of this type, a Li/Mn cation ordering, which leads to the subgroup *Cccm*, is not observed [49]. $LiNaMnS_2$, in which both *A* cations are small and which analogously belongs to the h.c.p. type

family, also exhibits a statistical occupation of Li and Mn at the tetrahedral voids of the respective aristotype $CaAl_2Si_2$ (Fig. 5, left). The complex new structure of the two mixed compounds $Na_2(K/Rb)MnTe_3$, which exhibit the formula of a metallate(III) containing edge-sharing dimers, contains Mn^{II} besides ditelluride ligands in addition to Te^{2-} and thus represents a basically new class of chalcogenido manganates. Nevertheless, the structure – among other anions – contains chains similar to those of the common K_2ZnO_2-type structure. The strong buckling of the chains in $Na_2(K/Rb)MnTe_3$, which exhibit a similar charge as the linear chains in A_2MnQ_2, again shows, that pure packing effects determine the shape of this structure motif; electronic contributions, atom pairing, charge ordering or magnetic interactions are not the reason for the strong differences in the shape of chalcogenido metallate chains (cf. discussion for the mixed-valent ferrates in [9]).

(iii) The structures of the *layered* ('phyllo') lithium and sodium chalcogenido metallates are fundamentally different from those of the larger alkali cations. *Li/Na*: The layered manganates(II) with the smaller lithium or/and sodium cations can be derived from the trigonal layers of tetrahedra in the $CaAl_2Si_2$-type structure: whereas the mixed-valent manganat(II/III) $NaMn_{1.56}Te_2$ show a statistical occupation of the tetrahedral voids in the aristotype, the manganates(III) $(Li/Na)MnSe_2$ [17] and $(Li/Na)MnTe_2$ [25] exhibit polar layers, in which only ½ of the tetrahedra of each layer are occupied, crystallographically leading to the t2 subgroup $P3m1$ (Fig. 5, left). In the mixed-valent phase $Na_3Mn_4Te_6$ Mn^{2+} cations occupy ⅔ of the tetrahedral voids between each second pair of hexagonal close packed Te layers. The monoclinic structure of space group $C2/m$ is thus again crystallographically related to the $CaAl_2Si_2$-aristotype (Fig. 5, left): the general t3 symmetry reduction from the trigonal (space group $P\bar{3}m1$) to the monoclinic *C*-centered crystal system ($C2/m$) is followed by a tripling of the monoclinic *b* axis, which allows to create the ⅓ empty tetrahedral voids along [010]. The crystallographic $a-b$ plane coincides with the manganate layers. In the likewise monoclinic *C* centered structure of $Na_2Mn_2S_3$ [16], $Na_2Mn_2Se_3$ [17] and the title compound $Na_2Mn_2Te_3$ a different ordering of a ⅔ occupation of the tetrahedral voids occurs. In this case, the unit cell contains two layers of tetrahedra along the stacking direction, which needs a doubling of *c* in the first step of a symmetry reduction. However, the observed *C* centering does not coincide with the former trigonal unit cell basis and there is consequently no direct group-subgroup relation between the $CaAl_2Si_2$ and the $Na_2Mn_2S_3$ structure. Only a metric transformation, which was already discussed in [16], can be quoted (cf. Fig. 5).

For $Na_2Mn_3Se_4$ [18] and the tellurium analogue $Na_2Mn_3Te_4$, the Se/Te arrangement consists of $3^6.4^2$ nets (cf. Fig. 1 in Sec. 3.1). Therefore, these two special compounds, which contain $[MnQ_6]$ octahedra in addition the the common $[MnQ_4]$ tetrahedra, can be denoted 'intermediates' between the h.c.p./$CaAl_2Si_2$ (3^6 nets) and the $ThCr_2Si_2$ (4^4 nets) structure family.

K-Cs: The layered manganates of the larger cations K^+, Rb^+ and Cs^+ are ordered defect variants of the tetragonal $ThCr_2Si_2$/PbO-type layers. Comparable to Li/Na manganates(III), the removal of ½ of the tetrahedra of the aristotype (t2 symmetry reduction from $I4/mmm$ to $I\bar{4}m2$) leads to the $TlAgTe_2$-type structure of the manganates(III) $AMnQ_2$ (A = K, Rb, Cs; Q = Se, Te; [17, 24]). A chain-like occupation of the tetrahedral voids by Mn and Na leads to the tetragonal structure of $CsNaMnTe_2$ (cf. above and Fig. 5). The group-subgroup relations associated with the ¾ occupation of the tetrahedra in the $Cs_2Mn_3S_4$-type structure of the Rb and Cs salts $A_2M_3Q_4$, which have long been known for the whole chalcogen series S/Se/Te, were described by Bronger et al. in [21]. Equally, the symmetry relation of the singular monoclinic structure of the potassium analog $K_2Mn_3S_4$ to the $Cs_2Mn_3S_4$- and the $ThCr_2Si_2$-type was already pointed out by this group [19].

4 Summary and outlook

The two tellurido manganates $Na_2Mn_2Te_3$ and $Na_2Mn_3Te_4$ are isotypic to the respective selenides and round out the series of pure sodium metallates(II) containing layered structures with a h.c.p. of chalcogenide ions. Whereas the Mn^{II} ions in $Na_2Mn_2Te_3$ occupy only tetrahedral voids, $Na_2Mn_3Te_4$ exhibits the rare octahedral coordination of Mn in addition. The two mixed alkali manganates Na_2AMnTe_3 (A = K, Rb) crystallize in a new complex orthorhombic structure consisting of buckled chains resembling the chains in the common compounds A_2MnQ_2, isolated ditelluride anions Te_2^{2-} and chains of alternately edge- and vertex-sharing $[MnTe_4]$ tetrahedra with one η^1-ditellurido ligand. These three anions are arranged in two different layers, which both reflect the compounds overall composition (**B**: $2\times[MnTe_{4/2}]^{2-} + Te_2^{2-}$; **A**: $[Mn_2Te_2Te(Te_2)Te_{2/2}]^{6-}$). The layers are separated by Na–(K/Rb) nets. The alkali coordination numbers are adjusted to the different sizes of the cations, leading to distinct positions of the two cation types and a fixed 2:1 composition of Na:K/Rb. Attempts to obtain the analogous Na/Cs compound yielded the 1:1 phase $NaCsMnTe_2$ instead. Its new

orthorhombic structure contains Cs^+ in a cubic eight-fold coordination and linear chains $[MnTe_{4/2}]$ fused to parallel chains $[NaTe_{4/2}]$. Therewith, the structure is an ordered derivative $Cs[NaMnTe_2]$ of the $ThCr_2Si_2$-type. Similar (if possible also crystallographic group-subgroup) relations to the basic structure types $CaAl_2Si_2$ (h.c.p. chalcogen packing, pure Li/Na salts) and $ThCr_2Si_2$ (nine-fold *Q* packing, K/Rb/Cs salts) are discussed for the new and all literature reported alkali manganates(II) and (III).

Even though the attempts to synthesize new mixed-valent manganates(II/III) were thus not yet successful, the title compounds obtained suggest a reinvestigation of the alkali chalcogenido-metallates of other two-valent metals like e.g. Zn, Cd and Hg. In the respective ternary systems A–M^{II}–Q many phases related to A_6MnQ_4 (A = Na–Cs), the different layered Na chalcogenido manganates(II) and in particular compounds with di-chalcogenido ligands are still missing.

Acknowledgements: We would like to thank the Deutsche Forschungsgemeinschaft for financial support.

References

[1] K. Preis, *J. Prakt. Chem.* **1869**, *107*, 12.
[2] W. Bronger, *Angew. Chem., Int. Ed. Engl.* **1981**, *20*, 52.
[3] M. R. Harrison, M. G. Francesconi, *Coord. Chem. Rev.* **2011**, *255*, 451.
[4] P. Stüble, S. Peschke, D. Johrendt, C. Röhr, *J. Solid State Chem.* **2018**, *258*, 416.
[5] M. Schwarz, C. Röhr, *Inorg. Chem.* **2015**, *54*, 1038.
[6] P. Stüble, A. Berroth, C. Röhr, *Z. Naturforsch.* **2016**, *71b*, 485.
[7] P. Stüble, C. Röhr, *Z. Anorg. Allg. Chem.* **2017**, *643*, 1462.
[8] W. Bronger, H. Balk-Hardtdegen, D. Schmitz, *Z. Anorg. Allg. Chem.* **1989**, *574*, 99.
[9] M. Schwarz, M. Haas, C. Röhr, *Z. Anorg. Allg. Chem.* **2013**, *639*, 360.
[10] W. Bronger, U. Ruschewitz, P. Müller, *J. Alloys Compd.* **1995**, *218*, 22.
[11] W. Bronger, M. Kimpel, D. Schmitz, *Angew. Chem., Int. Ed. Engl.* **1982**, *21*, 544.
[12] P. Stüble, J. Kägi, C. Röhr, *Z. Naturforsch.* **2016**, *71b*, 1177.
[13] W. Bronger, H. Balk-Hardtdegen, *Z. Anorg. Allg. Chem.* **1989**, *574*, 89.
[14] W. Bronger, M. Böhmer, P. Müller, *J. Alloys Compd.* **2002**, *338*, 116.
[15] M. Langenmaier, T. Rackl, D. Johrendt, C. Röhr, *Z. Naturforsch.* **2018**, *73b*, 837.
[16] K. Klepp, P. Böttcher, W. Bronger, *J. Solid State Chem.* **1983**, *47*, 301.
[17] J. Kim, T. Hughbanks, *J. Solid State Chem.* **1999**, *146*, 217.
[18] C. Pak, V. O. Garlea, V. Yannello, H. Cao, A. F. Bangura, M. Shatruk, *Inorg. Chem.* **2019**, *58*, 5799.
[19] W. Bronger, M. Böhmer, D. Schmitz, *Z. Anorg. Allg. Chem.* **2000**, *626*, 6.
[20] E. A. Axtell, J. Hanko, J. A. Cowen, M. G. Kanatzidis, *Chem. Mater.* **2001**, *13*, 2850.
[21] W. Bronger, H. Hardtdegen, M. Kanert, P. Müller, D. Schmitz, *Z. Anorg. Allg. Chem.* **1996**, *622*, 313.
[22] W. Bronger, U. Hendriks, P. Müller, *Z. Anorg. Allg. Chem.* **1988**, *559*, 95.
[23] J. A. Luthy, P. L. Goddman, B. R. Martin, *J. Solid State Chem.* **2009**, *182*, 580.
[24] J. Kim, C. Wang, T. Hughbanks, *Inorg. Chem.* **1999**, *38*, 235.
[25] J. Kim, C. Wang, T. Hughbanks, *Inorg. Chem.* **1998**, *37*, 1428.
[26] A. Benmakhlouf, A. Bentabet, A. Bouhemadou, A. Benghia, *J. Magn. Magn. Mater.* **2016**, *399*, 179.
[27] A. Benmakhlouf, A. Bentabet, A. Bouhemadou, S. Maabed, A. Benghia, R. Khenata, S. Bin-Omran, *J. Magn. Magn. Mat.* **2016**, *408*, 199.
[28] M. Langenmaier, C. Röhr, *Z. Kristallogr. Suppl.* **2017**, *37*, 113.
[29] K. Yvon, W. Jeitschko, E. Parthé, *J. Appl. Crystallogr.* **1977**, *10*, 73.
[30] G. M. Sheldrick, *Acta Crystallogr.* **2008**, *A64*, 112.
[31] G. M. Sheldrick, SADABS, *Program for Empirical Absorption Correction of Area Detector Data*, University of Göttingen, Göttingen (Germany) **2008**.
[32] X-SHAPE (version 1.03), *Crystal Optimization for Numerical Absorption Correction*, STOE & Cie GmbH, Darmstadt (Germany) **2005**.
[33] G. M. Sheldrick, SHELXS-97, *Program for the Solution of Crystal Structures*, University of Göttingen, Göttingen (Germany) **1997**.
[34] G. M. Sheldrick, SHELXL-97, *Program for the Refinement of Crystal Structures*, University of Göttingen, Göttingen (Germany) **1997**.
[35] CCDC 1922197 ($Na_2Mn_2Te_3$), 1922198 ($Na_2Mn_3Te_4$), 1922199 (Na_2KMnTe_3), 1922200 ($Na_2RbMnTe_3$), and 1922201 ($NaCsMnTe_2$) contain the supplementary crystallographic data for this paper. These data can be obtained free of charge from the Cambridge Crystallographic Data Centre via www.ccdc.cam.ac.uk/data_request/cif.
[36] L. M. Gelato, E. Parthé, *J. Appl. Crystallogr.* **1990**, *A46*, 467.
[37] V. Petříček, M. Dušek, L. Palatinus, JANA2006. *The Crystallographic Computing System*, Institute of Physics, Praha (Czech Republic) **2006**.
[38] L. W. Finger, M. Kroeker, B. H. Toby, *J. Appl. Crystallogr.* **2007**, *40*, 188.
[39] R. D. Shannon, *Acta Crystallogr.* **1976**, *A32*, 751.
[40] M. F. Mansuetto, J. A. Ibers, *J. Solid State Chem.* **1995**, *117*, 30.
[41] C. Graf, A. Assoud, O. Mayasree, H. Kleinke, *Molecules* **2009**, *14*, 3115.
[42] P. Stüble, A. Berroth, F. Wortelkamp, C. Röhr, *Z. Naturforsch.* **2019**, *74b*, 33.
[43] S. J. Ewing, M. L. Romero, J. Hutchinson, A. V. Powell, P. Vaqueiro, *Z. Anorg. Allg. Chem.* **2012**, *638*, 2526.
[44] M. S. Devi, K. Vidyasagar, *J. Chem. Soc. Dalton Trans.* **2002**, 4751.
[45] H. Bärnighausen, *MATCH, Commun. Math. Comput. Chem.* **1980**, *9*, 139.
[46] U. Müller, *Z. Anorg. Allg. Chem.* **2004**, *630*, 1519.
[47] M. I. Aroyo, J. M. Perez-Mato, C. Capillas, E. Kroumova, S. Ivantchev, G. Madariaga, A. Kirov, H. Wondratschek, *Z. Kristallogr.* **2006**, *221*, 15.
[48] R. Pöttgen, *Z. Anorg. Allg. Chem.* **2014**, *640*, 869.

[49] D. Schmitz, W. Bronger, *Z. Anorg. Allg. Chem.* **1987**, *553*, 248.
[50] W. Bronger, U. Hendriks, *Rev. Chim. Miner.* **1980**, *17*, 555.
[51] W. Bronger, *Angew. Chem., Int. Ed. Engl.* **1966**, *5*, 134.
[52] W. Bronger, P. Böttcher, *Z. Anorg. Allg. Chem.* **1972**, *390*, 1.
[53] K. Klepp, W. Bronger, *Z. Naturforsch.* **1983**, *38b*, 12.
[54] W. Bronger, C. Bomba, *J. Less-Common Met.* **1990**, *162*, 309.
[55] W. Bronger, C. Bomba, W. Koelmann, *Z. Anorg. Allg. Chem.* **1995**, *621*, 409.
[56] W. Bronger, W. Koelmann, P. Müller, *Z. Anorg. Allg. Chem.* **1995**, *621*, 412.